

# An Analysis of WFPC2 Filter Positional Anomalies

---

Shireen Gonzaga, Sylvia Baggett, John Biretta  
July 11, 2002

---

## ABSTRACT

*In March of 2001, a routine analysis of FR533N VISFLAT images revealed an anomaly: the filter wheel appeared to be offset by about  $0.42^\circ$  in some images. This offset angle is close to  $0.5^\circ$  degrees, which corresponds to one "filter step," (i.e., one increment in movement of the filter wheel by the filter electronics). These offsets are not a recent phenomena, and have been found in data as far back as mid-1994. This document describes a more exhaustive analysis of the filter wheel rotation anomaly: flatfield images for all available filters in the archive were inspected to determine if they exhibited similar behavior. Only filters that projected unique features (such as pinholes) onto the image were useful because these features were needed to detect the offsets. In addition to the previously-reported problem with FR533N, filter wheel rotation offsets have also now been found in these additional filter configurations: F375N, FR418N, FR533N18, FR533N33, FR533P15, FR680N, FR680N33, FQCH4N, FQCH4N15, and FQCH4P15. The offset angle was found to be  $0.42^\circ \pm 0.06^\circ$ . The occurrence rate of the offset error ranges from 0% to 40% for these filters (based on samples of 20 images or larger). It is also apparent that some filters (e.g. F160BW) show no rotation errors. In general, the errors will have little impact on GO science though photometric errors can reach a few percent in worst-case scenarios. There is also some hint that the problem may be getting worse with time. Currently, the cause of the anomaly is not completely understood. Cycle 10 and cycle 11 calibration programs will continue monitoring these filter wheel offsets.*

---

## Introduction

There are 48 filters in the WFPC2, mounted on 12 rotating filter wheels. Each wheel has 4 filters and one clear aperture referred to as the “home” position. The filter wheels are mounted in the Selectable Optical Filter Assembly (SOFA) that is located between the shutter and the reflecting pyramid.

In March of 2001, a problem was found with the FR533N filter in wheel 12. It was uncovered during a routine check of gain ratios over time using FR533N VISFLATs. A plot of the gain ratios revealed a rather bizarre feature: anomalous quantized values above and below the main gain ratio values (figure 1).

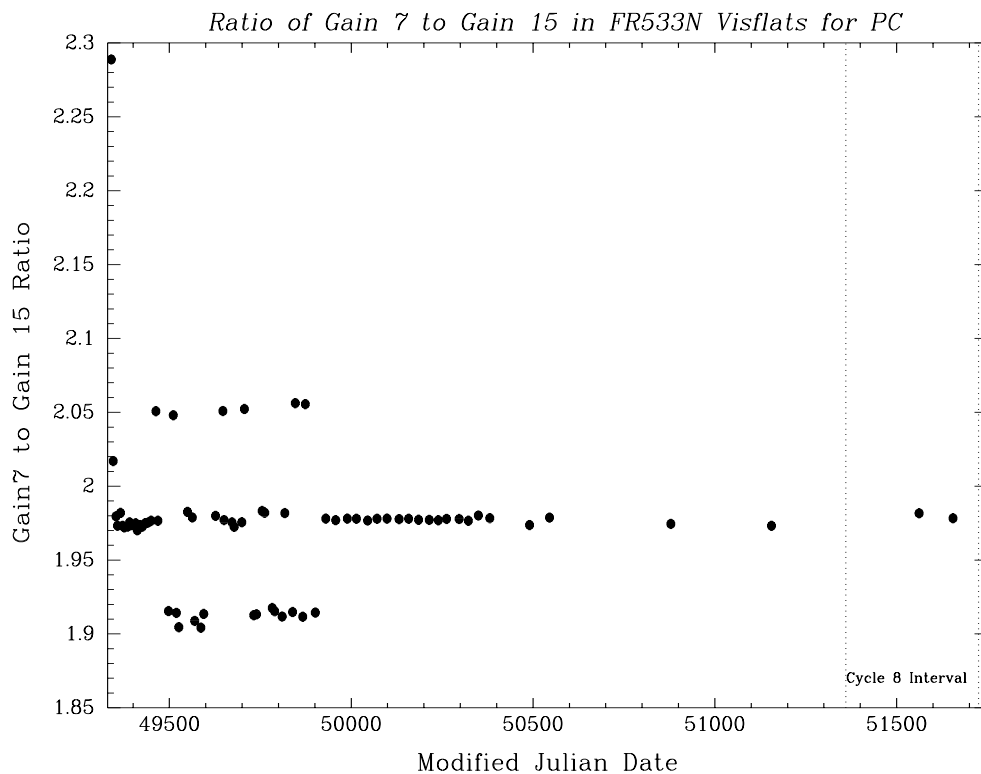


**Figure 1.** First hint of trouble: this plot of FR533N VISFLAT Gain 7 to Gain 15 Flux Ratios vs. Modified Julian Date, in the PC, revealed quantized values above and below the main gain ratio result.

The plot indicated that something was causing a change in the average count rate for some VISFLAT images. A visual inspection of those images revealed that FR533N filter pinhole features in some images appeared to be slightly offset compared to other images, as if some images had a slight rotational offset. Further analysis traced the problem to the FR533N filter wheel: the FR533N filter did not always land in its nominal position, instead it sometimes landed about  $0.5^\circ$  from its nominal position. This  $0.5^\circ$  offset corresponds to one “filter step,” a one increment of movement in the filter wheel by the filter

electronics. For more information about this preliminary study, please refer to Instrument Science Report WFPC2 2001-04: A Preliminary Assessment of the FR533N Filter Anomaly by Gonzaga et al. available at [http://www.stsci.edu/instruments/wfpc2/Wfpc2\\_isr/wfpc2\\_isr0104.html](http://www.stsci.edu/instruments/wfpc2/Wfpc2_isr/wfpc2_isr0104.html).

A more exhaustive check has since been done on other VISFLAT, INTFLAT, and Earthflat images to see if such offsets occur in other filters, and to obtain better measurements of the offset angle. Only filters that project filter features on their images, such as patterns, sharp edges and pinholes, were used because these features were necessary to detect filter wheel rotation offsets.

Note: We were unable to determine a nominal position for the filters from the images, and there was no engineering data available to make this determination. Therefore, when we refer to “filter wheel rotation offsets” in this document, we are describing offsets relative to an arbitrarily-selected reference image from a particular filter/target pool of images.

### **An Evaluation of all WFPC2 Filters**

Samples of Earthflat, VISFLAT, and INTFLAT images for all available filters were retrieved from the archive. Sample images for each filter/target configuration were inspected to determine if any filter features were present; only these images are useful to hunt for filter wheel rotation offsets. Useful filter features include filter pinholes (figure 2A), filter edges (figure 2B), and patterns unique to a particular filter (figures 2C & 2D).

For each filter/target configuration where filter features were present in the images, all available datasets were retrieved from the archive. Each set of images were checked to see if filter wheel rotation offsets were present. For the most part, this was done by simply “blinking” each image in a filter/target set with respect to an arbitrarily-selected reference image from that pool.

In many cases, there were a wide range of countrates within each image set that required the images to be normalized to an arbitrarily-selected reference image before being “blinked.” Some normalized images were also divided by the reference image to see if residuals revealed the presence of an offsets. However, this technique proved difficult for several reasons:

1. Cloud streaks in Earthflats varied from image to image.
2. There were also very slight feature variations in VISFLATS and INTFLATS, even in those taken close in time.
3. Due to the deteriorating VISFLAT lamp, VISFLATS spaced by long time intervals produced different countrates for the same exposure times.

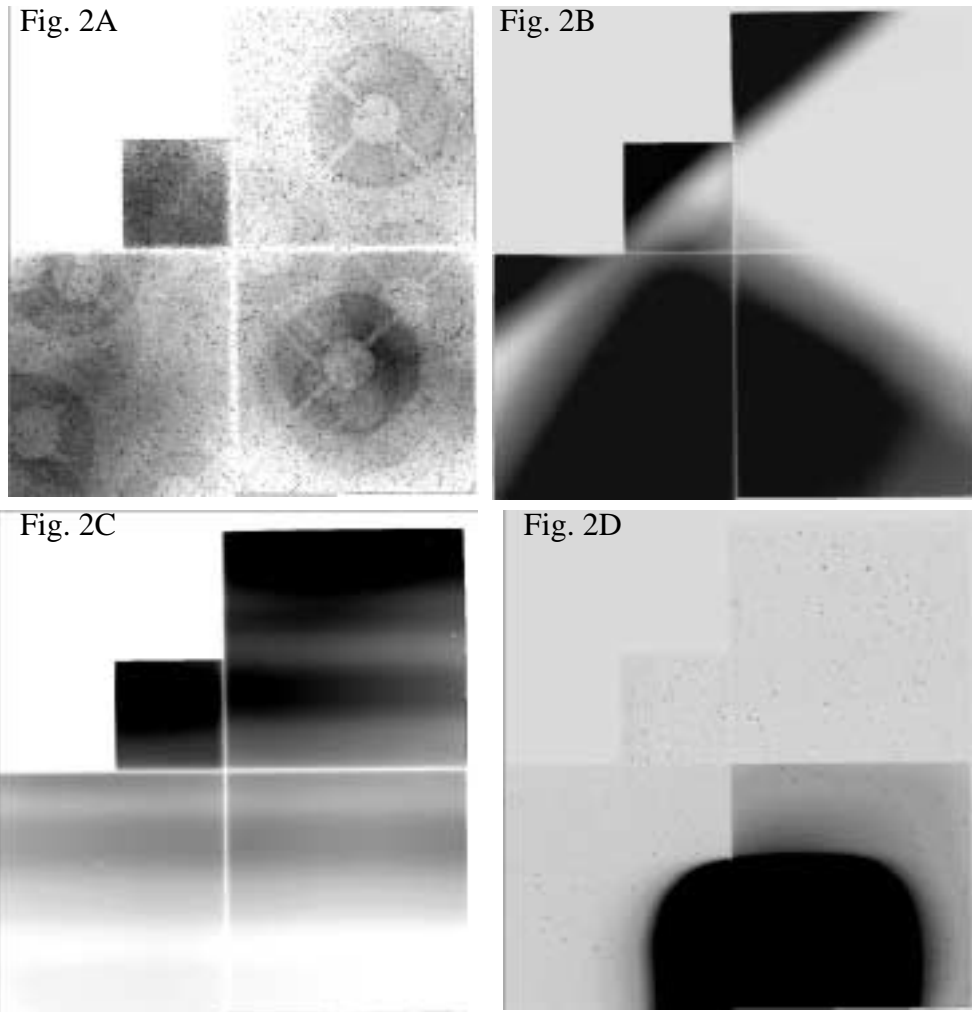


**Figure 2.** These mosaic'd images illustrate the three main categories of filter features that were used to determine if filter rotation was present.

**Figure 2A** (*u3iz1301t*) is an INTFLAT taken with the F390N filter, showing pinhole features.

**Figure 2B** (*u3i96604m*) shows well-defined filter edges in an Earthflat image taken with filters F502N x POLQN33 (where the features are mostly from POLQN33).

**Figures 2C and 2D** are examples of ramp filter features. Figure 2C (*u69q290ar*) is a VIS-FLAT image taken with FR533N, and figure 2D (*u6ak0704r*) is an Earthflat taken with the FR868N x F953N filters (with FR868N being the main contributor to the filter features).

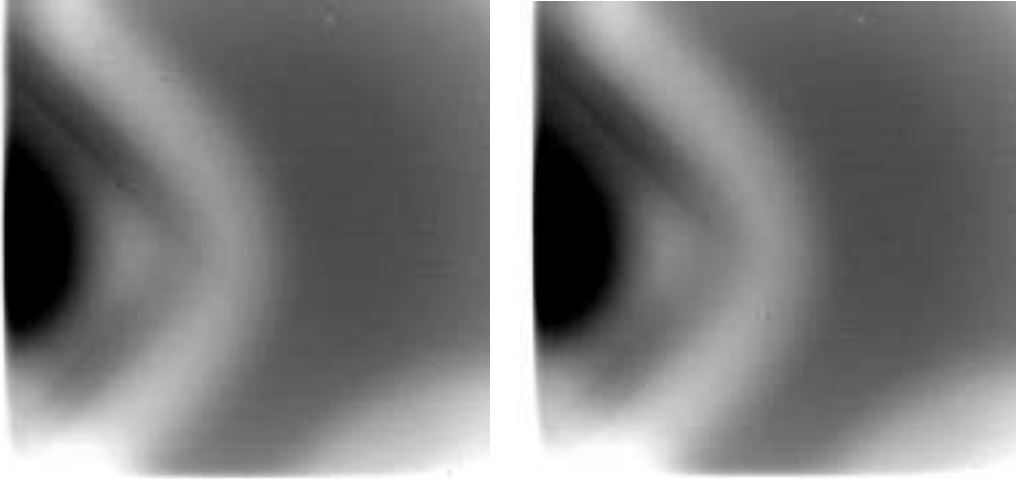


**Figure 3.** These two WF3 VISFLAT images, *u2es0905t* and *u2es0h05t* respectively, were taken with the FQCH4N filter. Most of the offset can be seen along the horizontal axis.

The following tables represent a summary of all available filter/target configurations examined. In cases where filter features were present, all available images for that particular configuration were retrieved from the archive to search for filter features shifted with respect to each other.

**Table 1:** Summary of results for Earthflat images

Filter1 (wheel,slot)	Filter2 (wheel,slot)	Filter Features	# Images Checked	# Images Shifted	% Images Shifted
F170W (8,1)	NULL	None	few	-	-
F185W (8,2)	NULL	None	few	-	-
F218W (8,3)	NULL	None	few	-	-
F255W (8,4)	NULL	None	few	-	-
F336W (3,1)	NULL	None	few	-	-
F343N (5,1)	NULL	None	few	-	-
F375N (5,2)	NULL	None	few	-	-
F390N (5,3)	NULL	None	few	-	-
F437N (5,4)	NULL	None	few	-	-
F469N (6,1)	NULL	None	few	-	-
F487N (6,2)	NULL	None	few	-	-
F502N (6,3)	NULL	None	few	-	-
F631N (7,1)	NULL	None	few	-	-
F656N (7,2)	NULL	None	few	-	-

Instrument Science Report WFPC2 2002-04

<b>Filter1 (wheel,slot)</b>	<b>Filter2 (wheel,slot)</b>	<b>Filter Features</b>	<b># Images Checked</b>	<b># Images Shifted</b>	<b>% Images Shifted</b>
F658N (7,3)	NULL	None	few	-	-
F673N (7,4)	NULL	None	few	-	-
F953N (1,1)	NULL	None	few	-	-
F502N (6,3)	FR533P15 (12,2)	Diffuse pattern in WF2	9	1	11.1%
F502N (6,3)	POLQ (11,1)	None	few	-	-
F502N (6,3)	POLQN18 (11,1)	None	few	-	-
F502N (6,3)	POLQN33 (11,1)	Filter edges in all chips	50	0	0%
F502N (6,3)	POLQP15 (11,1)	Diffuse pattern w/ filter edge in WF2&WF3	50	0	0%
F375N (5,2)	FR418N (12,1)	Diffuse pattern in WF4	9	2	22.2%
F437N (5,4)	FR418N (12,1)	Diffuse pattern in WF2	10	4	40.0%
F502N (6,3)	FR533N18 (12,2)	Diffuse pattern in WF2	20	4	20.0%
F502N (6,3)	FR533N (12,2)	Diffuse pattern in WF2	19	8	42.1%
F502N (6,3)	FR533N33 (12,2)	Diffuse pattern in WF2	9	2	22.2%
F588N (6,4)	FR533N33 (12,2)	Diffuse pattern in WF3	8	2	25.0%
F631N (7,1)	FR680N (12,3)	Diffuse pat- terns in WF3	20	8	40.0%
F673N (7,4)	FR680N (12,3)	Diffuse pattern in WF2	12	3	25.0%
F953N (1,1)	FR868N (12,4)	Diffuse pattern in WF2&WF3	20	0	0%

**Table 2:** Summary of results for INTFLAT images

<b>Filter 1 (wheel,slot)</b>	<b>Filter 2 (wheel,slot)</b>	<b>Filter Features</b>	<b># Images Checked</b>	<b># Images Shifted</b>	<b>% Images Shifted</b>
F1042M (11,2)	NULL	None	few	-	-
F300W (9,4)	NULL	All chips dif- fuse w/streaks. Pinholes in WF2&WF3	4	0	0%
F336W (3,1)	NULL	None	few	-	-
F380W (9,1)	NULL	None	4	-	-
F390N (5,3)	NULL	All chips diffuse, pin- holes in WF2,WF3 &WF4	4	0	0%
F410M (3,2)	NULL	None	4	-	-
F437N (5,4)	NULL	None	few	-	-
F439W (4,4)	NULL	None	few	-	-
F450W (10,4)	NULL	None	4	-	-
F467M (3,3)	NULL	None	4	-	-
F469N (6,1)	NULL	None	4	-	-
F487N (6,2)	NULL	None	4	-	-
F502N (6,3)	NULL	None	few	-	-
F547M (3,4)	NULL	None	few	-	-
F555W (9,2)	NULL	None	few	-	-
F569W (4,2)	NULL	None	few	-	-
F588N (6,4)	NULL	None	4	-	-
F606W (10,2)	NULL	None	few	-	-
F622W (9,3)	NULL	None	few	-	-
F631N (7,1)	NULL	Faint pinhole in PC	22	0	0%
F656N (7,2)	NULL	None	few	-	-
F658N (7,3)	NULL	None	4	-	-
F673N (7,4)	NULL	None	few	-	-
F675W (4,3)	NULL	None	few	-	-
F702W (10,3)	NULL	None	few	-	-
F785LP (2,3)	NULL	None	few	-	-

Filter 1 (wheel,slot)	Filter 2 (wheel,slot)	Filter Features	# Images Checked	# Images Shifted	% Images Shifted
F791W (4,1)	NULL	None	4	-	-
F814W (10,1)	NULL	None	few	-	-
F850LP (2,4)	NULL	None	4	-	-
F953N (1,1)	NULL	None	4	-	-

**Table 3:** Summary of results for VISFLAT images

Filter 1 (wheel,slot)	Filter 2 (wheel,slot)	Filter Features	# Images Checked	# Images Shifted	% Images Shifted
F1042M (11,2)	NULL	None	few	-	-
F160BW (1,2)	NULL	Pinholes in WF2, WF3, WF4	76	0	0%
F300W (9,4)	NULL	All chips diffuse, pinholes in WF2,WF3 &WF4	34	0	0%
F336W (3,1)	NULL	None	few	-	-
F375N (5,2)	NULL	All chips diffuse, pinholes in WF2,WF3 &WF4	24	3	12.5%
F380W (9,1)	NULL	None	few	-	-
F390N (5,3)	NULL	None	few	-	-
F410M (3,2)	NULL	None	few	-	-
F437N (5,4)	NULL	None	few	-	-
F439W (4,4)	NULL	None	few	-	-
F450W (10,4)	NULL	None	few	-	-
F467M (3,3)	NULL	None	few	-	-
F469N (6,1)	NULL	None	few	-	-
F487N (6,2)	NULL	None	few	-	-
F502N (6,3)	NULL	None	few	-	-
F547M (3,4)	NULL	None	few	-	-
F555W (9,2)	NULL	None	few	-	-
F569W (4,2)	NULL	None	few	-	-

Instrument Science Report WFPC2 2002-04

<b>Filter 1 (wheel,slot)</b>	<b>Filter 2 (wheel,slot)</b>	<b>Filter Features</b>	<b># Images Checked</b>	<b># Images Shifted</b>	<b>% Images Shifted</b>
F588N (6,4)	NULL	None	few	-	-
F606W (10,2)	NULL	None	few	-	-
F622W (9,3)	NULL	None	few	-	-
F631N (7,1)	NULL	None	few	-	-
F656N (7,2)	NULL	None	few	-	-
F658N (7,3)	NULL	None	few	-	-
F675W (4,3)	NULL	None	few	-	-
F702W (10,3)	NULL	None	few	-	-
F785LP (2,3)	NULL	None	few	-	-
F791W (4,1)	NULL	None	few	-	-
F814W (10,1)	NULL	None	few	-	-
F850LP (2,4)	NULL	None	few	-	-
F953N (1,1)	NULL	None	few	-	-
FQCH4N (11,4)	NULL	Unique filter pattern in all chips	15	4	26.7%
FQCH4N15 (11,4)	NULL	Unique filter pattern in WF2&WF3	6	1	16.7%
FQCH4N33 (11,4)	NULL	Unique filter pattern in WF2&WF3	6	0	0%
FQCH4NP15 (11,4)	BULL	Unique filter pattern in all chips	6	2	33.3%
FQUVN (11,3)	NULL	Diffuse, mostly WF2	15	0	0%
FQUVN33 (11,3)	NULL	Diffuse, filter edges in WF2&WF3	5	0	0%
FR418N (12,1)	NULL	Diffuse, pin- holes in WF2	6	2	33.3%
FR418N18 (12,1)	NULL	Diffuse, pin- holes in WF2	2	0	0%
FR418N33 (12,1)	NULL	Some diffuse features in WF2, WF3&WF4	2	0	0%
FR418P15 (12,1)	NULL	Diffuse streaks, pinholes in WF2	3	0	0%

Filter 1 (wheel,slot)	Filter 2 (wheel,slot)	Filter Features	# Images Checked	# Images Shifted	% Images Shifted
FR533N (12,2)	NULL	Diffuse streaks, pinhole in WF2,WF4	141	54	38.3%
FR533N18 (12,2)	NULL	Diffuse streaks	2	0	0%
FR533N33 (12,2)	NULL	Diffuse streaks, WF2,WF3& WF4	2	1	50%
FR533P15 (12,2)	NULL	Diffuse streaks, pinhole in WF4	2	1	50%
FR680N	NULL	Diffuse streaks	2	0	0%
FR680N18 (12,3)	NULL	Diffuse streaks	2	0	0%
FR680N33 (12,3)	NULL	Diffuse streaks	2	1	50%
FR680P15 (12,3)	NULL	Diffuse streaks	1	n/a	-
FR868N (12,4)	NULL	Diffuse streaks	2	0	0%
FR868N18 (12,4)	NULL	Diffuse streaks	2	0	0%
FR868N33 (12,4)	NULL	Diffuse streaks	2	0	0%
FR868P15 (12,4)	NULL	Diffuse streaks	1	n/a	-

### Filter Wheel Rotation Offset Measurements in Selected Filters

A filter wheel rotation offset can be determined by comparing each image in a pool of images using the same filter and target (Earthflat, VISFLAT or INTFLAT) configuration with an arbitrarily-selected reference image from that pool. The offset, if present, can be seen as a shift in the filter features when the image is blinked against the reference image. The offset angle can be determined from the amount of the shift and the distance of the shifted filter feature from the filter wheel rotation axis.

The distance of the filter wheel center (projected on the U2-U3 plane) to the center of the WFPC2 field-of-view is described in ISR WFPC2 96-05: Wavelength/Aperture Calibration of the WFPC2 Linear Ramp Filters) by Biretta et al., at [http://www.stsci.edu/instruments/wfpc2/Wfpc2\\_isr/wfpc2\\_isr9605.html](http://www.stsci.edu/instruments/wfpc2/Wfpc2_isr/wfpc2_isr9605.html).

An excerpt from that ISR:

*According to JPL blueprints of the filter wheel, the rotation axis is 2.165 inches above, and 0.704 inches left, of the filter cavity center, in a system where X and Y run parallel to the edge of the square of the filter cavity....*

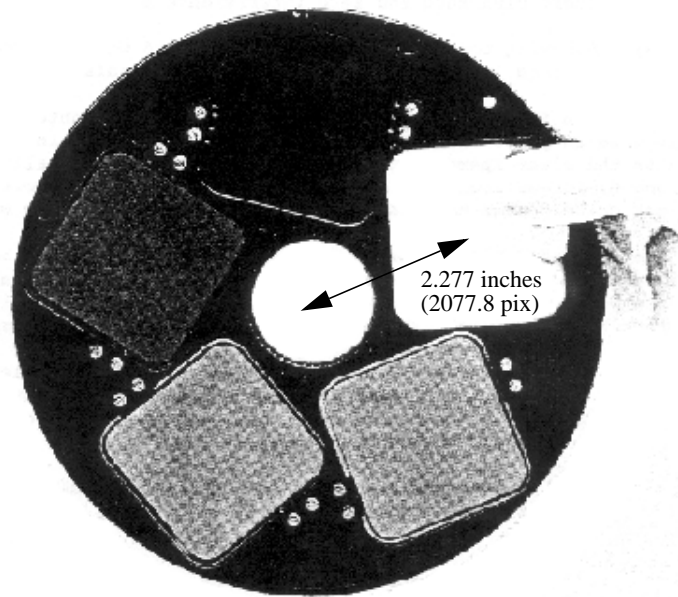


**Figure 4:** View of Filter Wheel showing filters in place. From the Wide Field Planetary Camera II Instrument Description and User Handbook, December 1993, issued by JPL.

These measurements give a distance from the filter cavity center (presumed to be the same as the WFPC2 field-of-view center) to the filter wheel rotation axis. However, the orientation of the filter wheel rotation axis with respect to the WFPC2 on the U-U3 plane was unavailable, and was determined by blinking shifted images and observing the direction of the shifts.

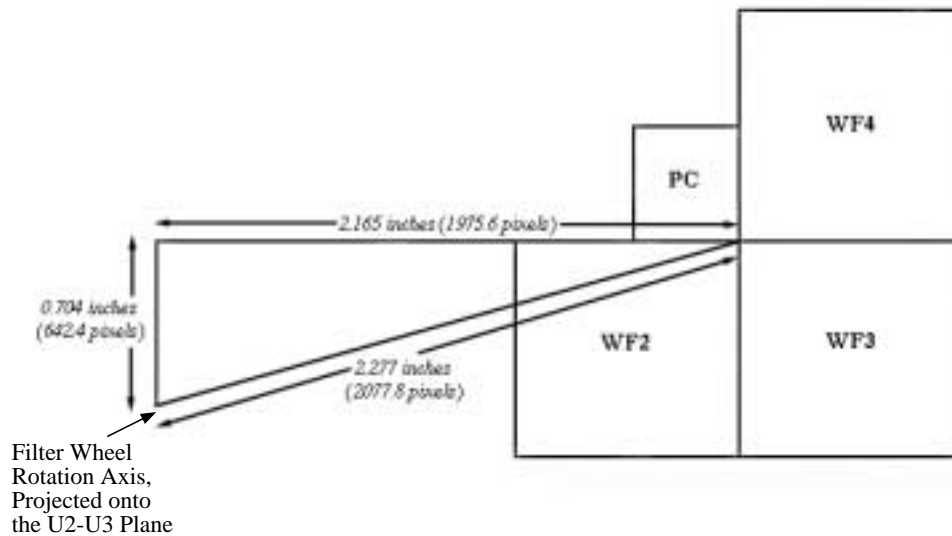


**Figure 5:** Location of the Filter Wheel Rotation Axis as projected onto the U2-U3 plane with respect to WFPC2 FOV.

Once the location of the filter wheel rotation axis on the U2-U3 plane was determined, it was possible to determine the filter rotation offset angle using the formula for the segment of a circle:

$$\theta = 2 \operatorname{asin}\left(\frac{c}{2R}\right)$$

where

$\theta$  is the filter wheel rotation angle offset in two shifted images,

$c$  is the shift in pixels between features in the two shifted images ( $c = \sqrt{x^2 + y^2}$ ),  
 $R$  is the distance from the measured filter feature to the filter wheel rotation axis.

Note: This formulation assumes the shifts are due solely to rotation of the filter wheel. While long-term changes in the camera geometry can also produce shifts, these are expected to be only about 1 pixel in size.

We selected 3 representative samples to illustrate the techniques used to measure the rotation offset.

### 1. Measurements Based on Diffuse Features

The simplest but least precise measurements were made using flats with very diffuse features. In most cases, this was made difficult by variable light sources such as those in Earthflats. However, in many cases, the displacement in filter features could be seen by

simply blinking the images. By carefully setting the image stretch, it was possible to obtain crude measurements of the displacement along the axis with the biggest shift.

Attempts at dividing two offset images to determine the shift from residuals proved to be unsuccessful since even minor differences in brightness between the two filter features could make the divided image difficult to evaluate.

### Example 1

The images in figure 6 show two offset Earthflats images (u6ak1707r & u6ak4707r respectively) with filter features in WF2 from filters FR418N and F437N (the feature came primarily from FR418N). The filter feature is rather diffuse and there is quite a bit of flux variation in the bright region due to different cloud streak features (this is not visible in the printed image but clearly seen by displaying the image at a proper stretch). Crude measurements were obtained by simply blinking the images back and forth on the image display software (in this case, using *SAOimage*). Since most of the offset was along the y-axis, x-axis shifts were very small and are therefore ignored in this example. A total of 10 measurements were taken of these two images:

$$c = (13+12+10+12+12+11+13+14+13+12)/10 = 12.2 \pm 1.13 \text{ pixels}$$

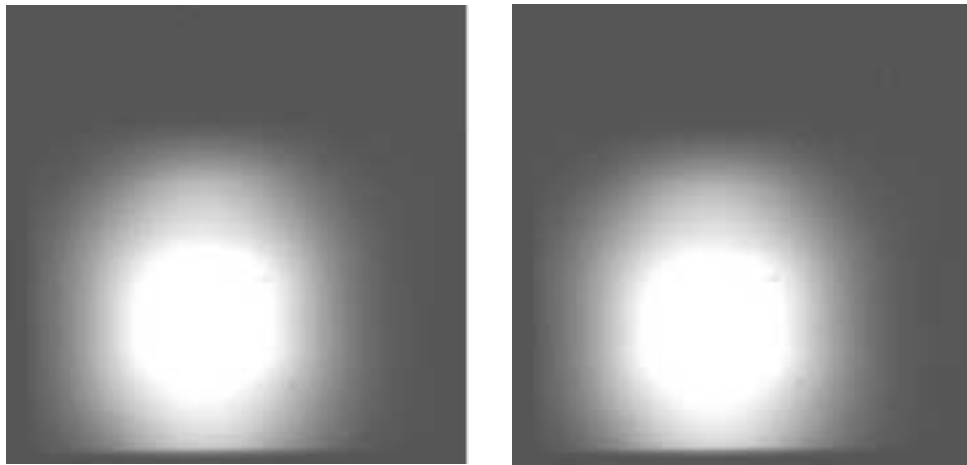


**Figure 6:** Two images (u6ak1707r & u6ak4707r) that are offset with respect to each other. These are filter features of Earthflats in WF2 taken with the FR418NxF437N filters.

Figure 7 illustrates how the y-axis displacement appears in the WFPC2 field-of-view. The location of the measurements in the wmosaic'd image coordinate system was at about (460,665). The center of the WFPC2 field-of-view (determined from a wmosaic'd image) is at about (758,784). Therefore, the distance from the filter wheel rotation axis to the location where measurements were taken was found to be 1757.3 pixels ( $R$ ). Because the x-axis displacement is very small, it was ignored. The feature displacement along the y-axis, designated as  $c$ , was 12.2 pixels.

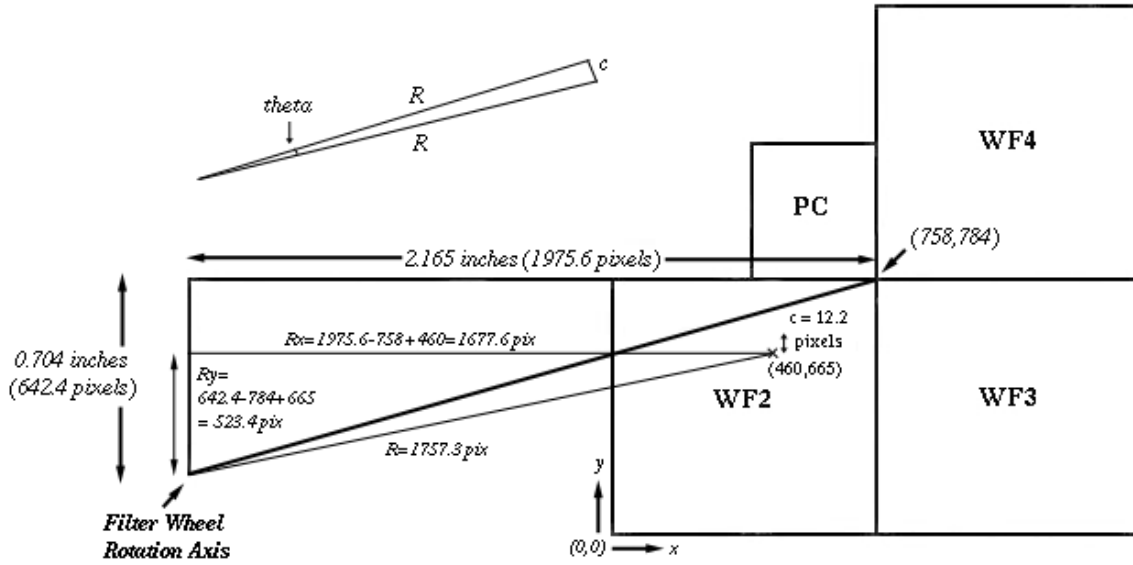


**Figure 7:** Location of image filter features in WFPC2 Field-of-View and filter wheel rotation axis in the U2-U3 plane.

$$\text{Therefore, } \theta = 2 \operatorname{asin}\left(\frac{c}{2R}\right) = 2 \operatorname{asin}\left(\frac{12.2}{2 \times 1757.3}\right) = 0.40^\circ$$

$$\begin{aligned} \text{In this figure, } Rx &= x + (1976 - 758) = x + 1218, \\ Ry &= y - (642 - 784) = y - 142, \\ R &= \sqrt{Rx^2 + Ry^2} \end{aligned}$$

Formal errors for the rotation offset value were around  $6 \times 10^{-4}^\circ$ . However, since  $c = 12.2 \pm 1.13$  pixels, the error in  $\theta$  due to measurements was  $0.04^\circ$ , yielding  $\theta$  between  $0.36^\circ$  and  $0.44^\circ$ , with the actual rotation offset value being actually larger since x-axis displacement was not included.

## 2. Measurements Based on Image Cross-sections

Another technique for measuring the shift between two images is to plot the flux in both images in the same columns or rows. Here, the IRAF task *pcols* was used to plot a vertical strip (averaged over columns 1110 to 1130) in two mosaic'd VISFLAT images taken with the FQCH4N filter. Because the two images are slightly offset from each other, a gap can be seen in the plot of the two images. Measuring the distance in pixels on the plot between two "points" that have the same flux gives the offset value (IRAF's *cursors* task was used to make measurements on the plot). This method can be somewhat subjective and thus more unreliable. The location for measurements has to be selected carefully.

It should be taken where the slope is steepest, which denotes a sharp brightness gradient where differences in flux that reveal the offsets can be seen most clearly.

**Example 2**

In this plot (figure 8), 5 measurements of the offset between the images (at positions where the flux value was the same) were taken at about (1120,700). As in the previous example, measurements were only taken along the axis where the largest displacement occurred.

Therefore,  $c = (14.7+16.6+14.7+ 14.8 +15.6)/5 = 15.28 \pm 0.83$  pixels

And at (1120,700),  $R$  was measured and calculated to be 2403.7 pixels.

So

$$\theta = 2 \operatorname{asin}\left(\frac{c}{2R}\right) = 2 \operatorname{asin}\left(\frac{15.28}{2 \times 2403.7}\right) = 0.36^\circ$$

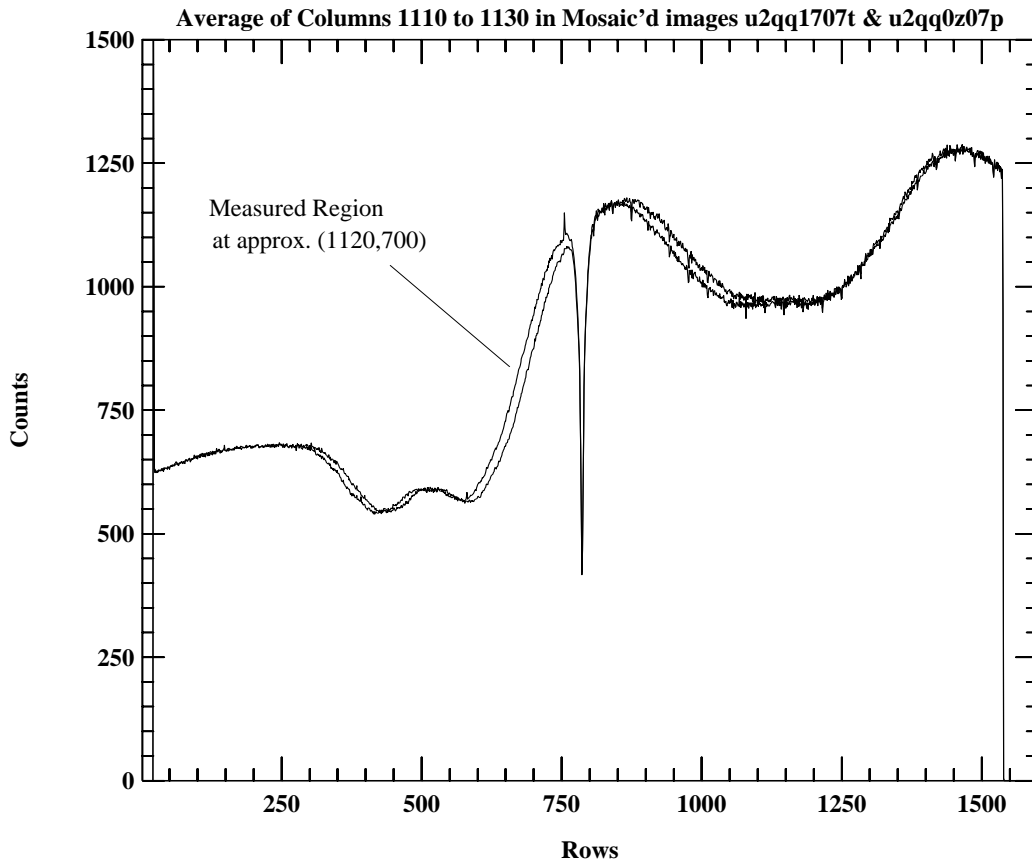


**Figure 8:** Plot of a vertical cross-section of two mosaic'd VISFLAT images taken using the FQCH4N filter. Measurements of the displacement between the two images were taken where the brightness gradient is greatest since it shows the offsets clearly.

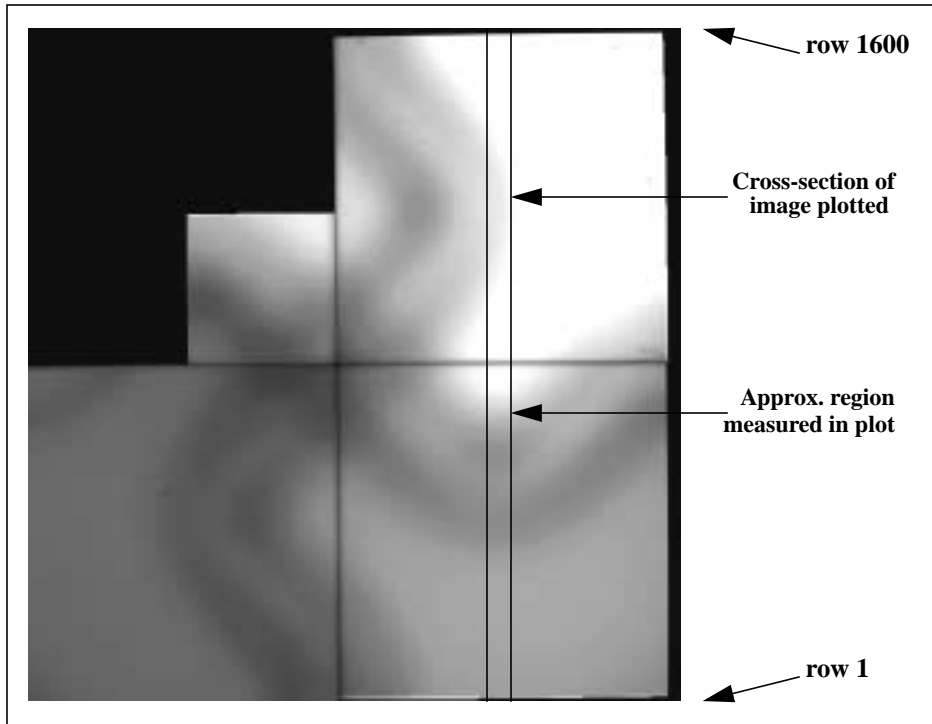


**Figure 9:** The mosaic'd VISFLAT FQCH4N image (u2qq0z07p) showing the image cross-section that was plotted in figure 8.

Since  $c = 15.28 \pm 0.83$  pixels,  $\theta$  is between  $0.34^\circ$  and  $0.38^\circ$ . And as in example 1, this value is likely a lower limit since motion along only one axis was considered.

### 3. Measurements Based on Filter Pinhole Positions

Some filters have well-defined features such as pinholes that project relatively sharp features on the flat-field images.

#### Example 3

In these F375N VISFLATs, positions of specific pinhole features (see figure 10) were measured in the two offset images, u232940t and u232930t.

Table 4 summarizes the measurements and range of values obtained for the filter wheel rotation offset from these two images. In the table,

$\Delta x$  is the offset in x-axis

$\Delta y$  is the offset in the y-axis

$c$  is the offset where  $c = \sqrt{\Delta x^2 + \Delta y^2}$

$R$  is the distance from the measured filter feature to the filter wheel rotation axis

$\theta$  is the filter wheel rotation offset in degrees

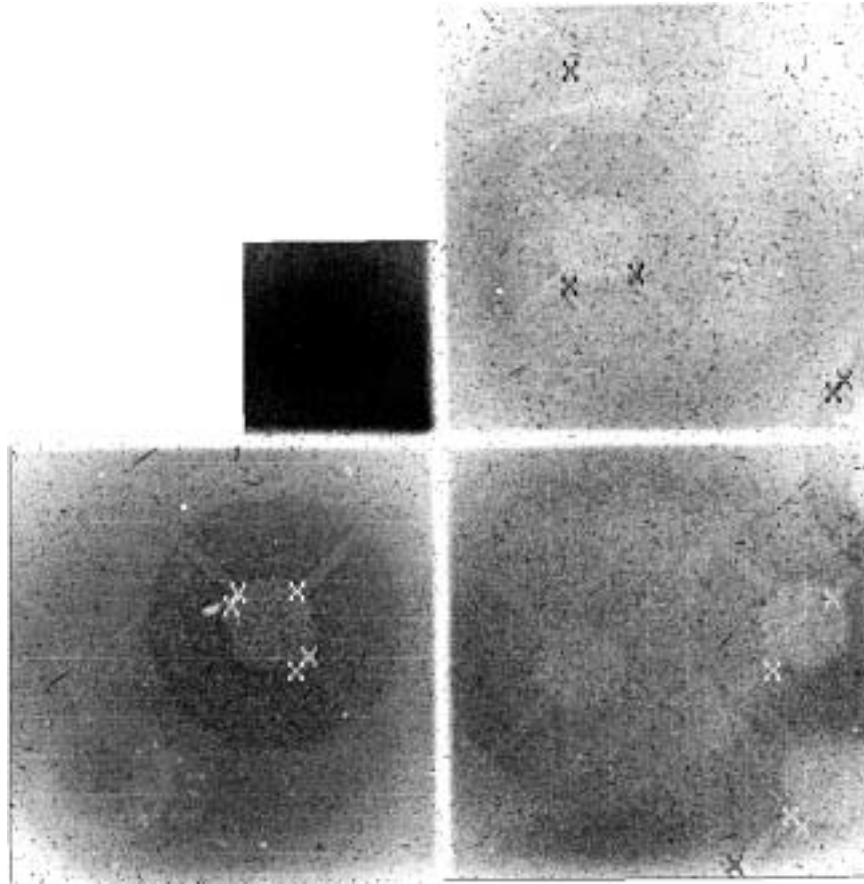


**Figure 10:** F375N VISFLAT image showing pinholes in WF2, WF3, and WF4. The measured regions are marked with X (in black or white).

**Table 4.** Summary of results for the filter wheel rotation offset using measurements in WF2, WF3, WF4 for two F375N VISFLATs.

Chip	Position in u232940t	Position in u232930t	$\Delta x$	$\Delta y$	$c$	$R$	$\theta$
WF2	400,495	396,510	4	15	15.52	1656.06	0.54
WF2	412,517	412,527	0	10	10	1672.58	0.34
WF2	514,520	510,532	4	12	12.65	1772.77	0.41
WF2	512,382	510,398	2	16	16.12	1746.57	0.53
WF2	535,407	528,420	7	13	14.76	1772.92	0.48
WF3	1370,130	1368,152	4	22	22.36	2588.03	0.49
WF3	1389,111	1391,130	2	19	19.11	2607.18	0.42
WF3	1338,382	1340,400	2	18	18.11	2567.24	0.40

Chip	Position in u232940t	Position in u232930t	$\Delta x$	$\Delta y$	$c$	$R$	$\theta$
WF3	1273,45	1268,62	5	17	17.72	2492.89	0.41
WF3	1443,508	1440,528	3	20	20.22	2686.05	0.43
WF4	986,1050	982,1065	4	15	15.52	2383.71	0.37
WF4	988,1423	980,1438	8	15	17	2550.96	0.38
WF4	1444,865	1444,883	1	18	18.03	2758.44	0.37
WF4	1463,887	1459,904	4	17	17.46	2782.59	0.36
WF4	1102,1071	1099 1090	3	19	19.23	2499.09	0.44

Based on these 15 measurements,  $\theta = 0.42^\circ \pm 0.06^\circ$ .

Measuring precise features on the pinholes was not trivial because of slight changes in the shape of the features from image to image. But in general, the presence of pinholes are helpful because their measurements appear to give the most accurate values for the filter wheel rotation offsets.

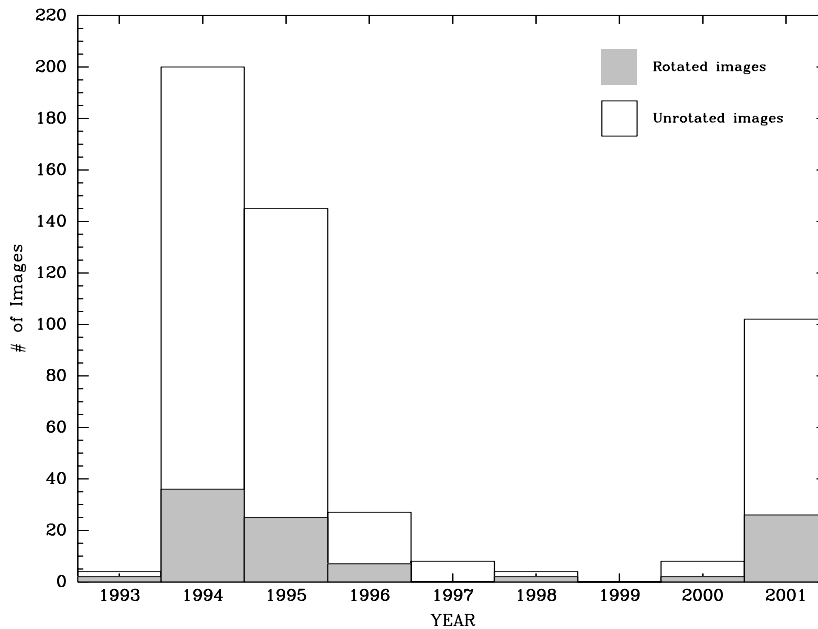
## Discussion

Table 5 summarizes our results for cases where 10 or more images were checked. A total of 15 filter combinations had 10 or more images checked. Of these, 88 out of 528 showed rotation errors, with the fraction of anomalous images ranging from 0% to 42.1% within the filter sets. It is also clear that some filters are not affected. For example, we checked 75 images taken with the F160BW filter, and none showed a rotation anomaly. We reiterate that table 5 only contains a small number of filters, only those with measurable features.

It is also interesting to consider whether the problem is growing worse with time. A histogram of filter rotation anomalies for each year from 1993 to 2001 (figure 11), as well as a breakdown of filter rotation image anomalies seen in each filter category (table 6), suggests that the problem could be worsening over time.

**Table 5:** Filter wheel anomaly statistics for image sets of 10 or more.

Target	Filter1 (wheel,slot)	Filter2 (wheel,slot)	# Images Checked	# Images Shifted	% Images Shifted
Earthflat	F502N (6,3)	POLQN33 (11,1)	50	0	0%
Earthflat	F502N (6,3)	POLQP15 (11,1)	50	0	0%
Earthflat	F437N (5,4)	FR418N (12,1)	10	4	40.0%
Earthflat	F502N (6,3)	FR533N18 (12,2)	20	4	20.0%
Earthflat	F502N (6,3)	FR533N (12,2)	19	8	42.1%
Earthflat	F631N (7,1)	FR680N (12,3)	20	8	40.0%
Earthflat	F673N (7,4)	FR680N (12,3)	12	3	25.0%
Earthflat	F953N (1,1)	FR868N (12,4)	20	0	0%
INTFLAT	F631N (7,1)	NULL	22	0	0%
VISFLAT	F160BW (1,2)	NULL	76	0	0%
VISFLAT	F300W (9,4)	NULL	34	0	0%
VISFLAT	F375N (5,2)	NULL	24	3	12.5%
VISFLAT	FQCH4N (11,4)	NULL	15	4	26.7%
VISFLAT	FQUVN (11,3)	NULL	15	0	0%
VISFLAT	FR533N (12,2)	NULL	141	54	38.3%



**Figure 11:** Frequency of filter rotation anomalies (shaded) compared to nominal images (not shaded) for each year from 1993 to 2001. The data is tabulated in tables 6 & 7.

# Instrument Science Report WFPC2 2002-04

**Table 6:** Breakdown of filter rotation image anomalies seen in each filter category, for each year, from 1993 to 2001. Table cells for the year columns are expressed in “Number of anomalous images / total number of images in the filter category.”  
 “/1” means that only one image existed for that filter category.

Filter(s)	Target	1993	1994	1995	1996	1997	1998	1999	2000	2001
F502N x FR533N	Earthflat	-	-	4/10	-	-	-	-	-	4/9
FR533N	VISFLAT	2/4	27/63	12/35	7/21	0/4	2/4	-	2/4	2/4
F502N x FR533N18	Earthflat	-	-	0/10	-	-	-	-	-	4/10
FR533N18	VISFLAT	-	-	/1	-	-	-	-	-	/1
F588N x FR533N33	Earthflat	-	-	-	-	-	-	-	-	2/8
F502N x FR533N33	Earthflat	-	-	2/9	-	-	-	-	-	-
FR533N33	VISFLAT	-	-	/1	-	-	-	-	-	/1
F502N x FR533P15	Earthflat	-	-	-	-	-	-	-	-	1/9
FR533P15	VISFLAT	-	-	-	-	-	-	-	-	0/2
F300W	INTFLAT	-	-	-	/1	/1	-	-	/1	/1
F300W	VISFLAT	-	0/28	0/6	-	-	-	-	-	-
F390N	INTFLAT	-	-	-	/1	/1	-	-	/1	/1
F631N	INTFLAT	-	0/2	0/4	0/4	0/4	-	-	0/4	0/4
F160BW	VISFLAT	-	0/40	0/33	0/2	/1	-	-	-	-
F375N	VISFLAT	-	3/24	-	-	-	-	-	-	-
FQCH4N	VISFLAT	-	3/10	1/5	-	-	-	-	-	-
FQCH4N15	VISFLAT	-	1/6	-	-	-	-	-	-	-
FQCH4N33	VISFLAT	-	0/6	-	-	-	-	-	-	-
FQCH4P15	VISFLAT	-	2/6	-	-	-	-	-	-	-
FQUVN	VISFLAT	-	0/10	0/5	-	-	-	-	-	-
FQUVN33	VISFLAT	-	0/5	-	-	-	-	-	-	-
F375N x FR418N	Earthflat	-	-	-	-	-	-	-	-	2/9
F437N x FR418N	Earthflat	-	-	-	-	-	-	-	-	4/10
FR418N	VISFLAT	-	-	0/2	-	-	-	-	-	2/4
FR418N18	VISFLAT	-	-	-	-	-	-	-	-	0/2
FR418N33	VISFLAT	-	-	-	-	-	-	-	-	0/2
FR418P15	VISFLAT	-	-	-	-	-	-	-	-	0/3
F631N x FR680N	Earthflat	-	-	4/10	-	-	-	-	-	4/10
F673N x FR680N	Earthflat	-	-	2/6	-	-	-	-	-	1/6

Filter(s)	Target	1993	1994	1995	1996	1997	1998	1999	2000	2001
FR680N	VISFLAT	-	-	/1	-	-	-	-	-	/1
FR680N18	VISFLAT	-	-	/1	-	-	-	-	-	/1
FR680N33	VISFLAT	-	-	/1	-	-	-	-	-	/1
FR680P15	VISFLAT	-	-	-	-	-	-	-	-	/1
F953N x FR868N	Earthflat	-	-	0/10	-	-	-	-	-	0/10
FR868N	VISFLAT	-	-	/1	-	-	-	-	-	/1
FR868N18	VISFLAT	-	-	/1	-	-	-	-	-	/1
FR868N33	VISFLAT	-	-	/1	-	-	-	-	-	/1
FR868P15	VISFLAT	-	-	-	-	-	-	-	-	/1
<b># Anomalous</b>	-	<b>2</b>	<b>36</b>	<b>25</b>	<b>7</b>	<b>0</b>	<b>2</b>	-	<b>2</b>	<b>102</b>
<b># Images Checked</b>	-	<b>4</b>	<b>200</b>	<b>145</b>	<b>27</b>	<b>8</b>	<b>4</b>	-	<b>8</b>	<b>26</b>
<b>% Anomalous</b>	-	<b>50.0</b>	<b>18.0</b>	<b>17.2</b>	<b>25.9</b>	<b>0</b>	<b>50.0</b>	-	<b>25.0</b>	<b>25.5</b>

**Table 7:** Filter rotation image anomalies seen in each filter wheel category, for each year, from 1993 to 2001. Note: Table contains “number of anomalous images/total number of images in the filter category”. Below it is the percentage of filter wheel rotation anomalies for each wheel, for each year from 1993 to 2000.

Wheel#	1993	1994	1995	1996	1997	1998	1999	2000	2001	Total
<b>1</b>	-	0/40 <b>0%</b>	0/33 <b>0%</b>	0/2 <b>0%</b>	-	-	-	-	-	0/75 <b>0%</b>
<b>5</b>	-	3/24 <b>12.5%</b>	-	-	-	-	-	-	-	3/24 <b>12.5%</b>
<b>7</b>	-	0/2 <b>0%</b>	0/4 <b>0%</b>	0/4 <b>0%</b>	0/4 <b>0%</b>	-	-	0/4 <b>0%</b>	0/4 <b>0%</b>	0/22 <b>0%</b>
<b>9</b>	-	0/28 <b>0%</b>	0/6 <b>0%</b>	-	-	-	-	-	-	0/34 <b>0%</b>
<b>11</b>	-	6/43 <b>13.9%</b>	1/10 <b>10.0%</b>	-	-	-	-	-	-	7/53 <b>13.2%</b>
<b>12</b>	2/4 <b>50.0%</b>	27/63 <b>42.9%</b>	24/92 <b>26.1%</b>	7/21 <b>33.3%</b>	0/4 <b>0%</b>	2/4 <b>50.0%</b>	-	2/4 <b>50.0%</b>	26/98 <b>26.5%</b>	90/290 <b>31.0%</b>

In JPL's Instrument Description and User Handbook, page E.1-5:

*Encoding the five filter positions is accomplished by first defining a home position. Home position is when the clear aperture is on the optical axis. Moving a filter wheel "home" is done by sensing an IR LED whose energy is reflected to an IR sensor by a small mirror on each wheel. The mirror is positioned so as to intercept the energy a little before home position (approximately 1/2 degree). Then, by way of a Schmidt trigger, the wheel is commanded to stop with a 200 msec damping pulse. It is then inched home by the electronics. From here on, any subsequent filter position (each being 72 degrees or 144 steps from each other) can be attained by commanding the electronics to supply  $N \times 144$  steps,  $N$  being the number of the desired filter position.*

This excerpt predicts a minimum possible offset angle of  $0.5^\circ$  ( $72^\circ/144$  steps =  $0.5^\circ$  per step). The filter offset anomaly may not be related to any particular filter, but to the "home" position electronics that drives the filter wheel. It's possible that the damping pulse that places the wheel at the home position is erratic and sometimes does not work, causing it to be off by 1 step ( $0.5^\circ$ ). In that case, however, one would expect all filters to be equally affected. But the lack of rotation seen in the F160BW images (wheel 1, 76 images checked) and F300W (wheel 9, 34 images checked) is difficult to explain. Assuming similar rates (20% - 40%) seen in other filters, one would have expected to find 15 to 30 rotation offsets out of the 76 F160BW images, and 7 to 14 rotation offsets out of the 34 F300W flats.

Another possibility, offered by Jesus (Sito) Balleza was: "Radiation degradation may be affecting the homing accuracy of the filters. The signal may be triggering past the one step in nominal position thus triggering the homing steps past the nominal position." (For more details, please see ISR 01-04: Preliminary Assessment of the FR533N Filter Anomaly, Gonzaga, et al. available at [http://www.stsci.edu/instruments/wfpc2/Wfpc2\\_isr/wfpc2\\_isr0104.html](http://www.stsci.edu/instruments/wfpc2/Wfpc2_isr/wfpc2_isr0104.html).)

To test this "one step from nominal" idea, we selected a pair of images that were offset with respect to each other: u2329301t and u2329401t, both F375N VISFLATS with pinhole filter features. Using the IRAF task *rotate*, image u2329401t was rotated  $0.5^\circ$  counter-clockwise about the filter wheel rotation axis to match it up with u2329301t. The two images were then blinked to see if they overlap. For a  $0.5^\circ$  rotation, there was still a slight offset between the images. So images rotated through a range of angles between  $0.4^\circ$  and  $0.45^\circ$ , in  $0.1^\circ$  increments, were compared to see which rotation would give the best overlap results. An exact match between images was hard to determine because of slight differences in the pinhole features between the images, but the best overlap between images occurred for rotation angles of  $0.41^\circ$  to  $0.43^\circ$ .

Our best measurements of the filter wheel rotation offset,  $0.42^\circ \pm 0.06^\circ$  (from example 3) does not match the integral filter wheel step of  $0.5^\circ$ . At this time, the reason for this difference is unknown.

**Figure 12A:** Location of WFPC2 image with respect to filter wheel rotation axis, projected onto the U2-U3 plane.

Filter Wheel  
Rotation Axis  
x

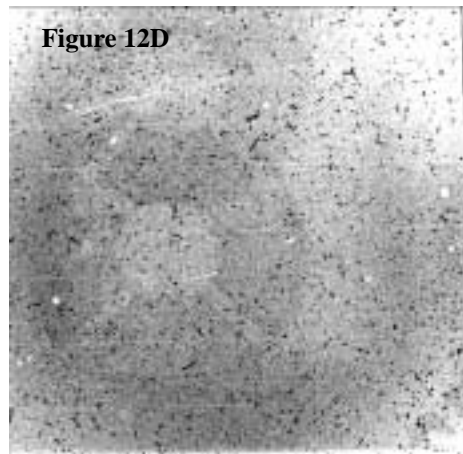
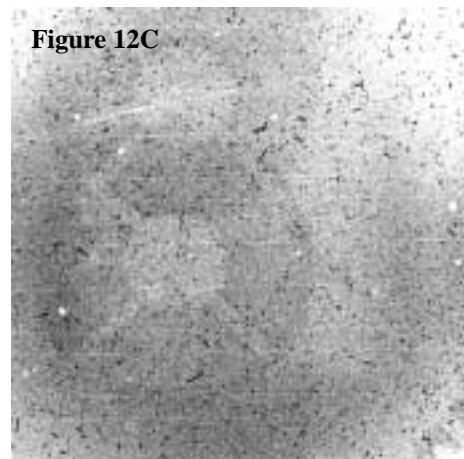
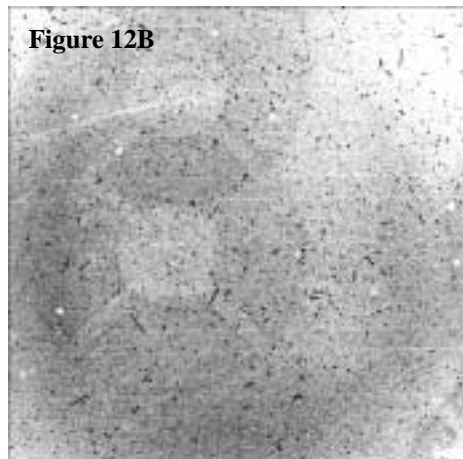
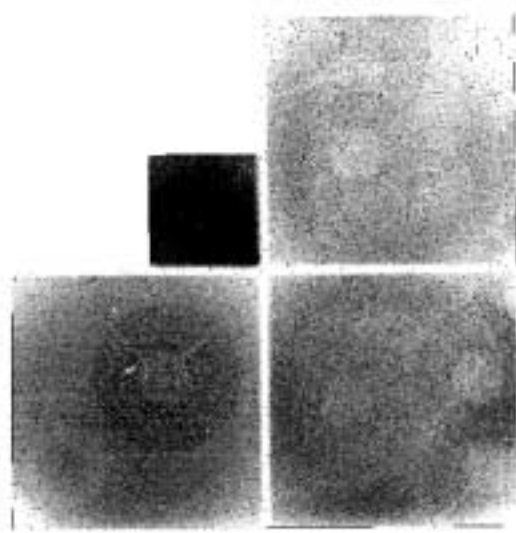


**Figure 12B** shows the WF4 image for u2329301t (F375N VISFLAT), which appears offset with respect to **figure 12C** (u2329401t). In **figure 12D**, u2329401t has been rotated counterclockwise by  $0.42^\circ$ . Blinking u2329301t with the rotated u2329401t shows a high degree of overlap in the filter pinhole features. This method of analysis indicates that the filter wheel rotation offset is between  $0.41^\circ$  and  $0.43^\circ$ .

## **Effects on Photometry**

### **F375N**

The F375N filter has strong filter features in the form of pinholes that are clearly seen in VISFLATs. Because the rotation anomaly can change the location of the filter features from one F375N image to another, the background can be affected for an object close to the edge of a filter feature.

For example, assume an object appears in two F375N images, where one image is affected by the filter wheel rotation anomaly and the other image is not. Both images were calibrated with the same flat field. If the object lies very close to, or on the edge of a filter feature in the first image, it will be displaced to another location with a different background in the second image, affecting the resulting photometry.

We examined twenty-four F375N VISFLATs, in WF2, WF3, and WF4, and obtained statistics for a small 20x20 pixel area inside a pinhole (brighter) region and another 20x20 pixel area in a uniformly illuminated area outside a pinhole (fainter) region. The mean flux ratio of these two regions would be the maximum effects possible on the sky determination as the edge of the filter feature moves across a source. In the WF2, the maximum difference in flux was 1.6% +/- 2%. For WF3 it was 4.9% +/- 0.8%, and for WF4, 2.2% +/- 1%.

### **FQCH4N, FQCH4N15, and FQCH4P15**

The FQCH4N (Methane Quad) can be partially rotated to provide coverage in other wavelengths in the WFPC2. For more details on how this filter works, please refer to the WFPC2 Instrument Handbook. Each “quad” has a unique central wavelength, believed to not vary significantly over the quad’s field-of-view (however, this is not known for certain and is currently being investigated). Therefore, the filter wheel rotation anomaly would only affect objects located near the vignetted areas of the filter.

### **FR418N, FR533N18, FR533N33, FR533P15, FR680N, FR680N33:**

Linear Ramp Filters (LRFs) are each made from four filter strips that vary in wavelength along the length of each strip. Each wavelength region, ranging from 3710 Å to 9762 Å over the four LRFs, is mapped to a particular position in the WFPC2 field-of-view. The four filters can also be used in a rotated mode. For more information about these filters, please refer to the WFPC2 Instrument Handbook.

The LRFs provide a 10” diameter unobstructed view (100 pixels in the WF, about 200 pixels in the PC) at a given wavelength. The primary effect of the rotation anomaly is displacement of this 10” diameter region on the WFPC2 detectors. A rotation error of 0.42° corresponds to about 20 pixels on WF3 and WF4, or about 2” motion of the 10” unvignetted diameter region; PC1 and WF2 experience smaller offsets, since they are closer to the pivot point. Hence, targets near the edges of the 10” region may experience

some vignetting if a rotation error occurs. However, the photometric effect of a 2" offset will be very small (less than 2%) since the OTA beam is about 34" in diameter at the LRF filter wheel.

The baseline linear ramp filter calibration analysis (in progress, Biretta & McMaster) shows that the photometry error is, on average, about 8%, with most of the error being in the negative range since the ramp filter throughput appears to be lower than expected. (This error estimate was obtained by comparing observed counts of the standard star GRW+70D5824 with predicted counts from Synphot.) Hence, the photometric error due to rotation is insignificant.

The rotation also causes a wavelength shift which we now examine. To assess how these wavelength shifts affect LRF photometry, we did two sample calculations at two extreme distances from the filter wheel rotation axis. The photometric error was found to range from 0.2% for a location in the WF2 near the filter wheel rotation axis, to 3% in the WF4, farthest away from the rotation axis where the offsets are largest. More typical errors due to wavelength shift are likely to be of order 1%. For details on how these photometry error estimates were made, please refer to Technical Instrument Report 02-05.

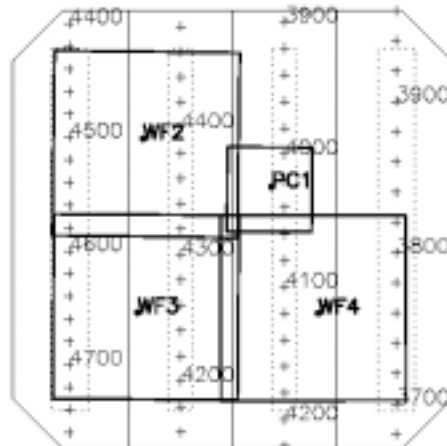


**Figure 13.** Example of how wavelengths are mapped onto the WFPC2 for the FR418N Filter.

**Acknowledgements:**

We would like to thank Stefano Casertano, Jesus (Sito) Balleza, Matt McMaster, J.C.Hsu, and Jessica Kim for their advice and contributions. And special thanks to Brad Whitmore for carefully reviewing the draft version of this ISR and providing many useful comments.

## References:

Wide Field Planetary Camera II Instrument Description and User Handbook, December 1993, issued by JPL.

Instrument Science Report 99-01: Internal Flat Field Monitoring II. Stability of the Lamps, Flats, and Gains, O'Dea, et al.

[http://www.stsci.edu/instruments/wfpc2/Wfpc2\\_isr/wfpc2\\_isr9901.html](http://www.stsci.edu/instruments/wfpc2/Wfpc2_isr/wfpc2_isr9901.html)

Instrument Science Report 96-05: Wavelength/Aperture Calibration of the WFPC2 Linear Ramp Filters) by Biretta et al.

[http://www.stsci.edu/instruments/wfpc2/Wfpc2\\_isr/wfpc2\\_isr9605.html](http://www.stsci.edu/instruments/wfpc2/Wfpc2_isr/wfpc2_isr9605.html)

Instrument Science Report WFPC2 2001-04: Preliminary Assessment of the FR533N Filter Anomaly by Gonzaga et al.

[http://www.stsci.edu/instruments/wfpc2/Wfpc2\\_isr/wfpc2\\_isr0104.html](http://www.stsci.edu/instruments/wfpc2/Wfpc2_isr/wfpc2_isr0104.html)

WFPC2 Handbook v6.1 (2002) by Biretta et al.

[http://www.stsci.edu/instruments/wfpc2/Wfpc2\\_hand/wfpc2\\_handbook.html](http://www.stsci.edu/instruments/wfpc2/Wfpc2_hand/wfpc2_handbook.html)

CRC Standard Mathematical Tables, 27th Edition. William H Beyer, editor. CRC Press 2000.